Enhancement of the Stabilisation Efficiency of a Neoclassical Magnetic Island by Modulated Electron Cyclotron Current Drive in the ASDEX Upgrade Tokamak

M.Maraschek,[1] G.Gantenbein,[2] Q.Yu,[1] H.Zohm,[1] S.Günter,[1]
F.Leuterer,[1] A.Manini,[1] ECRH group, and ASDEX Upgrade Team

[1]*Max-Planck-Institut für Plasmaphysik, EURATOM-Association, Boltzmannstr. 2, D-85748 Garching, Germany*
[2]*Forschungszentrum Karlsruhe, Association EURATOM-FZK, IHM, D-76021 Karlsruhe, Germany*

The efficiency of generating a helical current in magnetic islands for the purpose of suppression of Neoclassical Tearing Modes by Electron Cyclotron Current Drive is studied experimentally in the ASDEX Upgrade tokamak. It is found that the efficiency of generating helical current by continuous current drive in a rotating island drops drastically as the width $2d$ of the co-ECCD driven current becomes larger than the island width W. However, by modulating the co-ECCD in phase with the rotating islands O-point, the efficiency can be recovered. The results are in good agreement with theoretical calculations taking into account the equilibration of the externally driven current on the island flux surfaces. The result is especially important for large next-step fusion devices such as ITER, where $2d > W$ is expected to be unavoidable during NTM suppression, suggesting that modulation capability should be foreseen.

Introduction Neoclassical Tearing Modes (NTMs), i.e. magnetic islands generated by a loss of pressure driven current inside a toroidally confined fusion plasma, degrade plasma confinement above a certain pressure p at given magnetic field strength B_0. NTMs thus limit the achievable $\beta = \langle p \rangle / (B_0^2/(2\mu_0))$, which will be crucial for the economic viability of future fusion reactors. To overcome this limitation, schemes for the stabilisation of NTMs by local co - Electron Cyclotron Current Drive (co-ECCD) with respect to the plasma current have been developed [1–3]. Present experiments are usually performed with well-localised co-ECCD, i.e. the width $2d$ of the driven current is smaller than the marginal island size W_{marg} (for $W < W_{marg}$, a NTM naturally decays away). In this case, a continuous co-ECCD current is sufficient to efficiently suppress NTMs, because the redistribution of the current on the island flux surfaces generates *per se* a helical current component counteracting the loss of pressure driven current. In the opposite case $2d > W_{marg}$, theory predicts that continuous current drive will no longer generate helical current only inside the island [4] and therefore the stabilisation efficiency is drastically reduced. A possible way to overcome this suggested by theory is to modulate the co-ECCD current in phase with the magnetic island, depositing only around the O-point.

In this Letter, we report on an experimental verification of the loss of stabilisation efficiency with continuous co-ECCD at large d in the ASDEX Upgrade tokamak. We then show that by modulating the co-ECCD, we can recover a high stabilisation efficiency even at $2d > W_{marg}$. This experimental result is especially important for the planned ITER experiment, where it is expected that $2d > W_{marg}$ cannot be avoided due to the scaling of W_{marg} with poloidal ion gyroradius as opposed to the scaling of d with the absolute machine dimension.

Scan of the deposition width The deposition width and the driven current of the ECCD mainly depend on the toroidal launching angle ($|\Phi| > 0°$ for co-ECCD, $\Phi = 0°$ for pure heating). With the toroidal magnetic field B_t and the poloidal launching angle Θ the major radius R_{dep} of the ECRH deposition and the resonant surface can be controlled. Only B_t can be varied during the discharge, whereas Θ has to be fixed beforehand. Presently 3 gyrotrons depositing approximately 400kW each, with independent mirrors are available at ASDEX Upgrade. Typically Θ is adjusted in a way that the wave propagates through the plasma centre towards the deposition location on the high field side. The resonant surface is reached by a small scan of the magnetic field $B_t \approx -2.0T ... -2.3T$ towards higher absolute field.

Based on TORBEAM calculations [5] the resulting deposition width d, current density j_{ECCD}, total driven current I_{ECCD} and resulting current peaking I_{ECCD}/d are calculated. I_{ECCD}/d is shown in figure 1a. The deposition width d is the half width where $1/e$ of the maximum of j_{ECCD} is reached. The current peaking is normalised to the peak ECCD power P_{ECCD}^{max} and the ratio T_e/n_e in order to remove a variation of the driven current by different ECCD powers and different current drive efficiencies due to local plasma parameters. The marginal island size has been estimated to $W_{marg} \approx 3.5$cm. The condition $2d = W_{marg}$ is fulfilled for a torroidal launching angle of $\Phi \approx 13°$. It can be seen that for a range $\Phi \approx 2°...8°$ the highest current density, hence the highest I_{ECCD}/d, is reached at $2d/W_{marg} \approx 0.35$.

Additionally the normalised reduced island size W_{min}/W_{sat}(no ECCD) is shown. The minimal island size W_{min} during the ECCD pulse is normalised to the saturated island W_{sat}(no ECCD) size before the application of the ECCD. For pure heating ($\Phi = 0°$) and broad deposition with low I_{ECCD}/d ($\Phi \gtrsim 15°$) only a reduction to typically half the saturated island size is achieved (figure 4a). Only in the range $3° < \Phi \lesssim 15°$, complete stabilisation is possible for unmodulated ECCD.

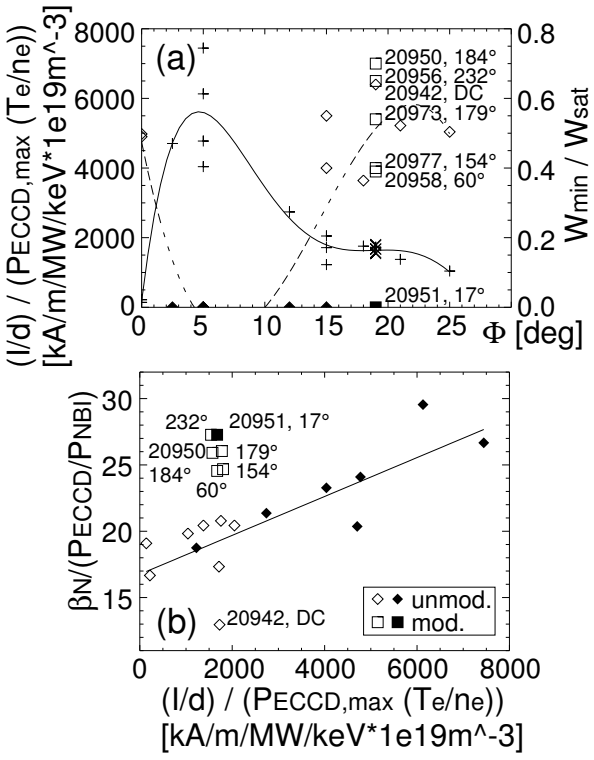

FIG. 1: (a) TORBEAM calculations of the width and total driven current. The ratio $(\frac{I_{ECCD}}{d})/(P^{max}_{ECCD}\frac{T_e}{n_e})$ as function of the toroidal launching angle Φ (+ for unmodulated, × for modulated , solid curve) is shown together with the achieved normalised minimal island size W_{min}/W_{sat}(no ECCD) of the (3/2)-NTM (diamonds and squares for unmodulated and modulated ECCD, filled for stabilised NTMs, broken curve for unmodulated ECCD only). (b) shows the maximal $\beta_N/(\frac{P_{ECCD}}{P_{NBI}})$ as function of $(\frac{I_{ECCD}}{d})/(P^{max}_{ECCD}\frac{T_e}{n_e})$ with the same symbols as in (a). Cases with modulated ECCD are indicated with shotnumbers and ECCD phase α_{exp}.

The achievable $\beta_N = \beta/(I_p/aB_t)$ normalised to P_{ECCD}/P_{NBI} is shown in figure 1b as function of $(\frac{I_{ECCD}}{d})/(P^{max}_{ECCD}\frac{T_e}{n_e})$. This describes the reachable β_N, i.e. the reachable pressure with stabilised or reduced NTM for an additionally applied amount of P_{ECCD} per injected background P_{NBI}. It can be clearly seen for unmodulated ECCD from the corresponding linear fit, that with increasing current peaking $(\frac{I_{ECCD}}{d})/(P^{max}_{ECCD}\frac{T_e}{n_e})$ (current density j_{ECCD}) the stabilisation gets more efficient. For a given P_{ECCD} a higher β_N can be reached, or a lower P_{ECCD} is required to reach a given β_N. Narrow deposition has also been applied for the (3/2)-NTM stabilisation in improved H-mode discharges. The NTM could be stabilised at the highest $\beta_N \approx 2.5$ at the lowest $q_{95} = 2.9$, i.e. roughly the ITER target, at ASDEX Upgrade to date, showing the possibility of NTM stabilisation at ITER q_{95} values. Experiments with unmodulated ECCD for the (2/1)-NTM show similar improvements [6].

Theoretical predictions for broad ECCD deposition First theoretical considerations on the requirement of a modulation for NTM stabilisation assumed the deposition width d of the ECCD to be smaller than the marginal island size W_{marg} [7, 8]. With $2d < W_{marg}$ modulation does not improve the efficiency of the ECCD significantly and has been no longer considered [1, 7, 9]. In the above presented cases with $2d > W_{marg}$ the maximal available ECCD power could no longer stabilise the (3/2)-NTM. Calculations for $2d > W_{marg}$ show, that the efficiency of ECCD stabilisation is significantly improved with modulation in the O-point of the island [9].

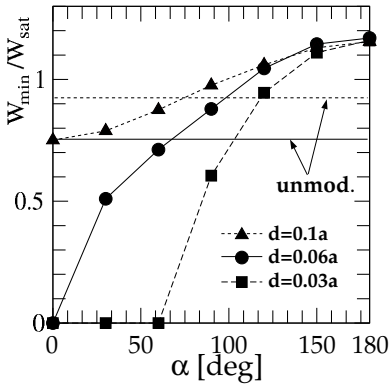

FIG. 2: Variation of the achievable island size with unmodulated and modulated ECCD (50% duty cycle) for different phasings ($\alpha = 0°$ for O-point, $\alpha = 180°$ for X-point). The deposition width has been assumed to be $d/a = 0.1, 0.06, 0.03$ for modulated and $d/a = 0.1, 0.06$ for unmodulated ECCD.

Calculations on the effect of the different phasings and duty cycles have been performed in order to gain a full understanding of the experimental findings. The deposition width normalised to the minor plasma radius has been varied over the values $d/a = 0.1/0.06/0.03$. The experiments have been performed with $d/a = 0.06$. The phase angle α in figure 2 corresponds to the phase of the modulated co-ECCD (with respect to the plasma current) pulses relative to the islands phase. The driven current is taken to be in the order of $I_{ECCD}/I_{plasma} = 0.02$, i.e. 2% of the total plasma current. The considered model presently ignores the heating effect on the stabilisation efficiency [9]. The effect of the fast electron collisionality ν is included, which governs the time it takes to build up the current in the O-point. For $\nu/\omega << 1$ it takes several tens of oscillations until the time averaged saturated ECCD current can be reached, where ω represents the angular frequency of the mode. For O and X-point phasing an stabilising and destabilising effect is predicted compared to the unmodulated case, respectively. A duty cycle of 50% is predicted to have the strongest effect for both phasings.

Modulated ECCD with broad deposition As shown above, with broad ECCD deposition ($\Phi > 15°$) the NTM can not be stabilised completely and the achievable

$\beta_N/(\frac{P_{ECCD}}{P_{NBI}})$ is reduced. By applying broad modulated co-ECCD with deposition around the islands O-point, complete stabilisation can be regained (figure 3).

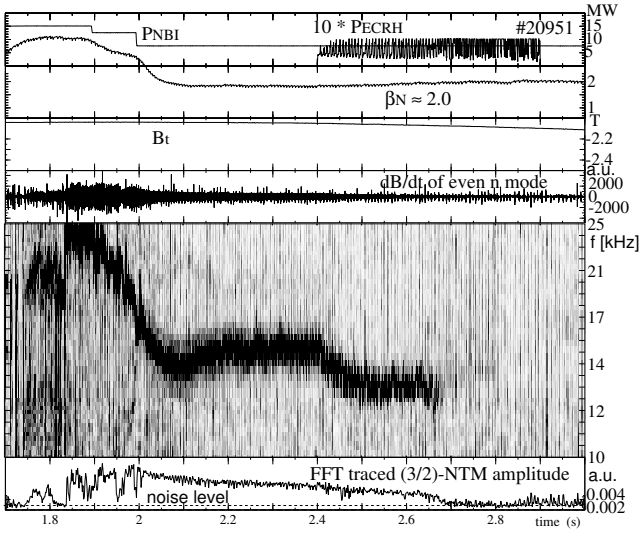

FIG. 3: Stabilisation of a (3/2)-NTM with broad modulated ECCD in the O-point of the island. The time traces show the heating power (P_{NBI}, modulated P_{ECCD}), β_N, the pre-programmed B_t-ramp, the n=2 filtered dB_{pol}/dt raw data, a spectrogram of the n=2 filtered magnetics and the FFT traced amplitude of the (3/2)-NTM. A complete stabilisation can be observed after 2.7s.

A direct comparison between 2 similar discharges clearly shows the improvement with O-point modulation (figure 3 and 4). In both cases the amplitude of the mode is initially reduced during the slightly adapted B_t-ramp when the ECCD moves radially into the island, but only in the modulated case the mode disappears and β_N recovers. In the unmodulated case β_N stays at values comparable to the time when the ECCD has not yet reached the resonant surface.

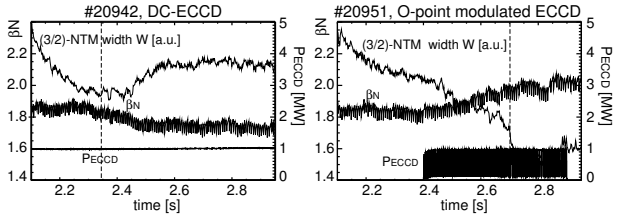

FIG. 4: Comparison between two nearly identical discharges with unmodulated (a) and modulated (b) broad ECCD deposition. Only the B_t-ramp has been slightly adapted to match the resonance condition between ECCD an the mode. The vertical dashed lines indicate the time when the resonance is reached and the minimum island size W_{min} is taken.

The data points for the modulated broad ECCD deposition are added in the diagrams in figure 1. The current peaking is comparable to the unmodulated cases. The island size reduction for $\Phi = 19°$ shows a variation from complete stabilisation for #20951 to worse stabilisation than for the unmodulated case #20942, depending on the phasing (next section). The improvement in $\beta_N/(\frac{P_{ECCD}}{P_{NBI}})$ in figure 1b shows two distinct groups for unmodulated and modulated discharges. For the unmodulated cases an improvement with increasing current peaking can be seen. For the modulated cases higher values in $\beta_N/(\frac{P_{ECCD}}{P_{NBI}})$ can be observed. This is due to the halved average ECCD power to reach the same β_N. At present no deposition width scan has been performed for modulated cases.

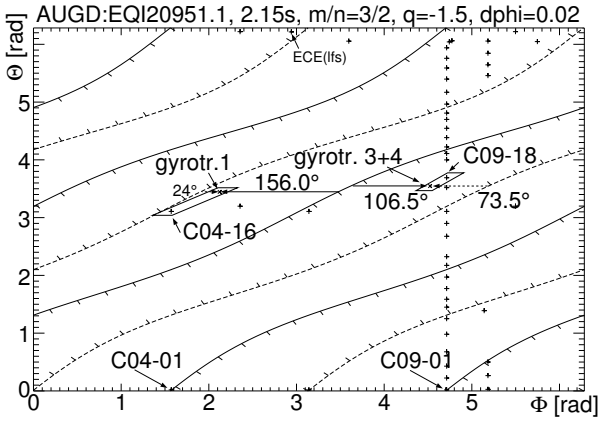

FIG. 5: Mapping between the ECCD deposition (× signs) from TORBEAM calculations and the location of the Mirnov probes (+ signs). The phase is set to the location of the reference coils (C09-01, C04-01). An independent phase control with the probes C04-16 and C09-18 for gyrotron 1 and 3,4, respectively, is possible due to their closeness to the ECCD.

Effect of the phasing of modulated ECCD In order to resolve the influence of the relative phase between the islands O-point and the deposited ECCD power, the ECCD has been modulated with different phases at $\Phi = 19°$, corresponding to $2d/W_{marg} \approx 1.6$. The phase of the mode has been determined by a linear combination of Mirnov coils measuring dB_{pol}/dt. For the modulation of the ECCD the sum of the signals of the coils C09-01 and C04-01 has been used for the amplitude of modes with even n-numbers. They are located 180° toroidally apart. This phase is mapped along the magnetic field line on the $q = m/n = 1.5$ resonant surface to the calculated co-ECCD deposition of gyrotrons 1 and 3+4 (figure 5). The resulting phase shift, also indicated in figure 5, corrects for each gyrotron the phase difference between the magnetic measurement and the co-ECCD deposition. This shift is applied to the controller for the modulation independently of the frequency of the mode.

Additionally the alignment of the ECCD deposition with the island can be compared independently with a subset of coils, which lie on the same magnetic field line. Coil C04-16 and coil C09-18 fulfil this condition for gyrotron 1 and for gyrotrons 3+4, respectively

(figure 5). The gyrotrons are injecting ECCD power in discharge #20951 (figure 6a) when these coils show $B_{pol}^{island} < 0$ ($d(dB_{pol}^{island}/dt)/dt > 0$). The poloidal field B_{pol}^{plasma} generated by the plasma current I_p is positive, i.e. $B_{pol}^{plasma} > 0$. The perturbation current within the island flows parallel to the plasma current in the X-point and antiparallel in the O-point. Consequently for the X-point $B_{pol}^{island} > 0$ and for the O-point $B_{pol}^{island} < 0$ holds. It becomes clear that the ECCD is indeed deposited in phase with the islands O-point.

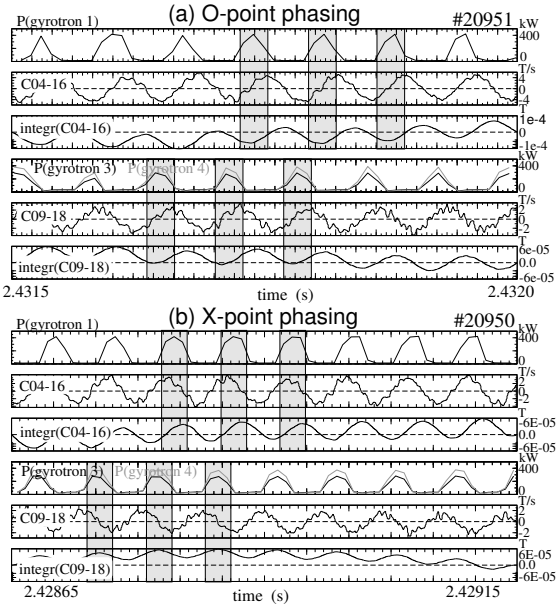

FIG. 6: Modulated ECCD power, dB_{pol}^{island}/dt of the reference coils (C04-16,C09-18) and the integrated B_{pol}^{island}. The suppressed offset $B_{pol}^{plasma} > 0$ is always positive. (a) For the O-point phasing of the ECCD stabilisation for broad deposition could be recovered. The shaded times indicate the ECCD during the $B_{pol}^{island} < 0$ phases for both gyrotron groups. (b) For the X-point phasing the smallest reduction of the island size has been observed. The shaded times indicate $B_{pol}^{island} > 0$ phases. Gyrotron 1 is not well aligned in this case.

Consequently for the inverted phasing with deposition centred around the X-point of the island ($B_{pol}^{island} > 0$) the smallest island size reduction is observed. In figure 1 discharge #20950 has the largest W_{min}/W_{sat}, i.e. the smallest island size reduction. Figure 6b shows the corresponding phasing close to the X-point.

The remaining discharges were performed with modulated ECCD with different phasings between O and X-point corresponding to a variation of the angle α in figure 2. Figure 7 shows the relative reduced island size W_{min}/W_{sat} as function of α_{exp}. This experimental phase α_{exp} represents an averaged phase over the two groups of gyrotrons relative to the control coils C09-01 and C04-01. The phase offset of $\approx 156°$ indicated in figure 5 has been corrected. Numerically the O-point case #20951 is not perfectly aligned to the O-point, as one can also see in figure 6a. The predicted behaviour in figure 2 could be perfectly reproduced. The predicted destabilising effect for pure X-point deposition could not be found. However, for near X-point phasing (discharges #20950 and #20956 in figure 7) a reduced stabilisation compared to unmodulated broad ECCD can be observed, due to the higher required accuracy for X-point phasing.

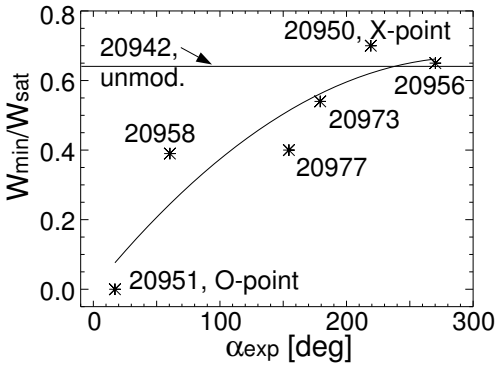

FIG. 7: Reduced island size W_{min}/W_{sat} as function of the gyrotron averaged ECCD phase α_{exp} corresponding to figure 2. The phase difference between the control coils and the gyrotrons is corrected in α_{exp}, as indicated in figure 5. A parabolic fit through the data points are indicated.

Summary and conclusions A comprehensive scan of the (3/2)-NTM stabilisation efficiency depending on the deposition width of the ECCD has been performed. This clearly shows the advantage of a narrow deposition ($2d < W_{marg}$) and the loss of the stabilisation capability for broad deposition ($2d > W_{marg}$). With narrow deposition a significant improvement in terms of achievable β_N or a reduction of the required ECCD power to achieve a desired β_N has been observed.

At ASDEX Upgrade it has been shown for the first time in a tokamak that the loss of stabilisation for broad ECCD can be recovered by modulation of the ECCD in phase with the islands O-point. These results suggest that in future large fusion experiments, such as ITER, modulation capability should be foreseen for NTM stabilisation.

[1] H. Zohm et al., Nucl. Fusion **39**, 577 (1999).
[2] A. Isayama et al., Plasma Phys. Controlled Fusion **42**, L37 (2000).
[3] R. J. La Haye et al., Phys. Plasmas **9**, 2051 (2002).
[4] C. C. Hegna et al., Phys. Plasmas **4**, 2940 (1997).
[5] E. Poli et al., Comput. Phys. Commun. **136**, 90 (2001).
[6] M. Maraschek et al., Nucl. Fusion **45**, 1369 (2005).
[7] G. Giruzzi et al., Nucl. Fusion **39**, 107 (1999).
[8] F. W. Perkins, et al., 24th EPS Conf., Berchtesgaden, **21A, part III**, 1017 (1997).
[9] Q. Yu et al., Phys. Plasmas **11**, 1960 (2004).